Direct Growth of Single-layer Terminated Vertical Graphene Array on Germanium by Plasma Enhanced Chemical Vapor Deposition

Abdulrahman Al-Hagri,[1,#] Ru Li ,[1,#] Nitul S Rajput,[1] Jin-You Lu,[1,3] Shan Cong,[2] Karen Sloyan,[1] Mariam Ali Almahri,[1] Srinivasa Reddy Tamalampudi,[1] Matteo Chiesa,[1,3*] and Amal Al Ghaferi[1,*]

[1]Laboratory for Energy and Nano Science, Masdar Campus, Khalifa University, Abu Dhabi, UAE

[2]Key Lab of Nanodevices and Applications, Suzhou Institute of Nano-Tech and Nano-Bionics, Chinese Academy of Sciences (CAS), Suzhou 215123, China

[3]Department of Physics and Technology, UiT The Arctic University of Norway, Tromsø, Norway.

* Corresponding authors: Tel:+971- 02 810 9144

E-mail: matteo.chiesa@ku.ac.ae (Matteo Chiesa), amal.alghaferi@ku.ac.ae (Amal Al Ghaferi)

[#]These authors contributed equally.

Abstract

Vertically aligned graphene nanosheet arrays (VAGNAs) exhibit large surface area, excellent electron transport properties, outstanding mechanical strength, high chemical stability, and enhanced electrochemical activity, which makes them highly promising for application in supercapacitors, batteries, fuel cell catalysts, etc. It is shown that VAGNAs terminated with a high-quality single-layer graphene sheet, can be directly grown on germanium by plasma-enhanced chemical vapor deposition without an additional catalyst at low temperature, which is confirmed by high-resolution transmission electron microscopy and large-scale Raman mapping. The uniform, centimeter-scale VAGNAs can be used as a surface-enhanced Raman spectroscopy substrate providing evidence of enhanced sensitivity for rhodamine detection down to 1×10^{-6} mol L^{-1} due to the existed abundant single-layer graphene edges.

1 Introduction

Vertically aligned graphene nanosheet arrays (VAGNAs), in which two-dimensional (2D) graphene nanosheets are grown perpendicularly to the substrates to construct a three-dimensional (3D) ordered and interconnected array structure with enriched edges of graphene sheets, have attracted increasing interests for their application in gas sensors,[1] biosensors,[2] electrocatalysts,[3] field electron emission,[4, 5] photothermal,[6] solar cell,[7] electric double-layer capacitors,[8] faradaic pseudocapacitors,[9, 10] lithium-ion batteries,[11] vanadium redox flow batteries[12, 13] and fuel cells[14] due to their abundant edges, open channels, large surface area, excellent conductivity and enhanced electrochemical activity.[15, 16] Plasma enhanced chemical vapor deposition (PECVD) has been used to grow VAGNAs on various substrates, including metals (Cu, Ni, W, Al, Ti, Pt, stainless steel), semiconductors (Si, Ge, GaAs) and dielectrics (SiO_2 and Al_2O_3).[17-22] In general, the growth of VAGNAs by PECVD is a complicated process, where the morphology, nanosheet size, crystallinity, phase composition, and adhesion are strongly influenced by gas composition, substrate biasing, pressure, applied plasma power, substrate temperature, growth time, and substrate type.[15] Typically, the VAGNAs grown by PECVD have a tapered structure, with few-layer graphene at the top and multilayer graphene at the bottom, standing perpendicular to the substrates.[17, 18, 21, 23] The carbon precursors,[24] gas ratio of CH_4/H_2,[18] dopants such as NH_3 or N_2,[25] and substrate bias[19] have been used to tune the morphology and structure. VAGNAs with a bi-

layered Raman feature have been obtained by fine tuning the gas ratio, temperature and plasma power.[5, 18] Keivan *et. al.* reported the direct growth of VAGNAs terminated by bi-layered graphene on Si/Au and Si/Ni substrates.[17] However, VAGNAs terminated by high-quality single-layer graphene has yet to be obtained.

In this work, we report the direct growth of large-area, uniform VAGNAs with a height of 30-190 nm via a PECVD approach at a low temperature of 625℃ on Ge substrate. In the literature, the mechanism of VAGNAs grown by PECVD has been discussed in the light of ion bombardment effect and directional electric field.[5, 26] At the beginning of the PECVD process, a defected multilayer graphene film as buffer layer will grow horizontally on the substrate, and then the graphene nanowall sheets will form in vertical configuration owing to the intense plasma-induced ion bombardment and electric field. The catalytic activity of Ge substrate[27, 28] plays a role at the beginning of the multilayer graphene film deposition, which in turn affects the quality of VAGNAs. The as-grown VAGNAs show a tapered structure with high-quality single-layer graphene termination, which is confirmed by high-resolution transmission electron microscopy (HR-TEM) and Raman mapping. It is found that the amorphous carbon deposited inside the PECVD chamber is critical for the growth of single-layer graphene. Furthermore, the VAGNAs can be employed as an efficient surface-enhanced Raman spectroscopy (SERS) substrate with detection sensitivity down to 1×10^{-6} mol L^{-1} rhodamine due to the ultra-clean surface and the abundant single-layer graphene edges.

2 Experimental

2.1 *PECVD growth of VAGNAs*

Synthesis of the VAGNAs was carried out by an Oxford PlasmaPro® 100 PECVD system, plasma was generated by an RF generator (13.56 MHz) close to the Ge surface (≤2 cm). 1 cm^2 undoped Ge<111> was cleaned by acetone, isopropanol and deionized water before growth. The PECVD chamber was heated to 625℃ under a flow of 20 sccm H_2. To grow the VAGNAs, 40 sccm CH_4, 60 sccm H_2, and 400 sccm Ar were ignited with a plasma power of 20-80 W at a pressure of 400 mTorr. The total growth time was 90 min. After growth, the system was cooled down to 250℃ with a flow of 20 sccm H_2 and 1000 sccm Ar.

2.2 *Characterization of VAGNAs*

AFM image was collected by a Cypher S system. SEM images were taken in a dual beam system (FEI Helios Nanolab 650). The tool was also used to prepare cross-sectional samples. Raman spectra were recorded with a WITec alpha300 R system with a laser wavelength of 532 nm at room temperature and under ambient conditions. The optical images were obtained using an Olympus BX51M optical microscope. The TEM analysis of the samples was done in a Titan G2 80-300 kV instrument operating at 80 kV. The system is also integrated with a Gatan Imaging Filter (GIF) for Electron energy loss spectroscopy (EELS) studies. TEM samples were prepared by spin-coating of PMMA on top of VAGNAs first, etching away Ge in HNO_3: HF: H_2O=1:1:3 solution, transferring PMMA/VAGNAs to a Quantifoil TEM grid and finally removing the PMMA by acetone.

2.3 *Raman enhancement measurement*

R6G ethanol solutions with concentration varying from 10^{-4} to 10^{-6} M were obtained from a stock solution of 10^{-3} M by successive dilution. Then, 50 μL of R6G solution with a given concentration was dropped on the substrate and was allowed to spread over the whole surface of the substrate spontaneously, followed by drying at room temperature for 2 hours in the dark. Raman spectra were subsequently acquired on a high-resolution confocal Raman spectrometer (LabRAM HR-800) with an excitation laser of 532 nm. The spectra were collected by using a ×50 L objective lens for 15 s with a laser spot diameter of about 1 μm and power of 0.3 mW for all acquisitions.

3 Results and discussion

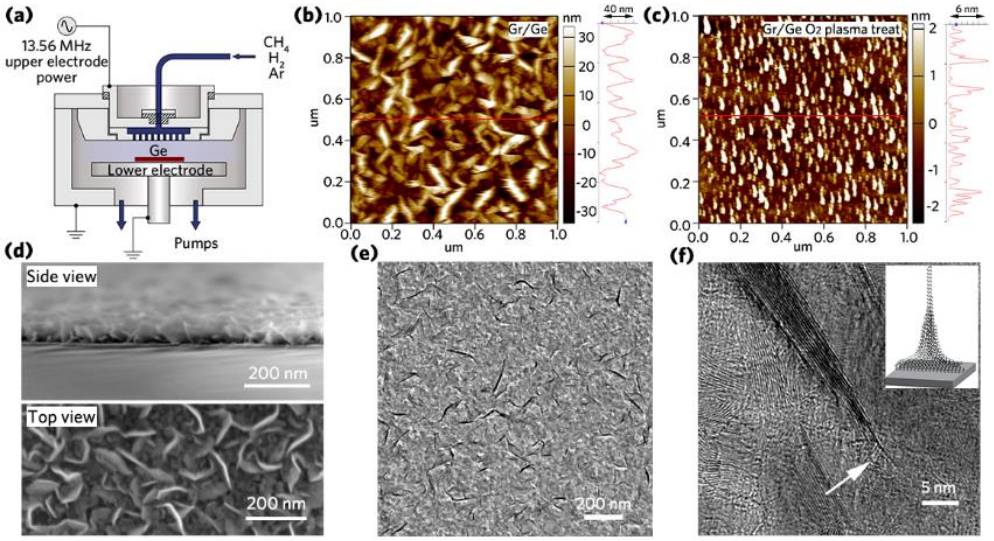

Fig. 1. VAGNAs grown on Ge substrate. (a) Schematic illustration of the PECVD system. AFM topography of VAGNAs (b) before and (c) after 20 min O_2 plasma treatment, and the corresponding cross-section profile indicated by the red line, respectively. (d) Side and top SEM view of the VAGNAs. (e) The TEM image of VAGNAs in front view. (f) High-resolution TEM of the tapered structure, single-layer graphene is indicated by an arrow, inset, the schematic illustration of the tapered structure.

The PECVD system for the growth of VAGNAs is schematically shown in Fig. 1a, where high purity methane (CH_4, 99.999%), hydrogen (H_2, 99.999%), and argon (Ar, 99.999%) were used as carbon precursor, etching agent, and carrier gas, respectively. A cleaned 1 cm^2 undoped Ge<111> was placed in the center of the lower electrode that acted as a heat plate. CH_4, H_2, and Ar were injected through a showerhead and plasma was generated by an RF generator (13.56 MHz). Since the plasma generator is close to the Ge surface (≤2 cm), which has a strong ion bombardment effect and results in a rough Ge surface at the growth temperature of 625℃. The roughness of Ge was measured by atomic force microscopy (AFM) after the VAGNAs was removed by 20 min oxygen (O_2) plasma treatment (Fig. 1c), where a maximum 6 nm height difference was observed. Additional experiments confirmed that the 20 min O_2 plasma treatment did not introduce extra roughness (Fig. S1, Supporting Information) and the VAGNAs was removed completely (Fig. S2). Fig. 1b shows the typical surface morphology of VAGNAs, where a maximum 40 nm height difference is observed, which is consistent with the typical 40-60 nm height VAGNAs. The side and top view of VAGNAs (Fig. 1d) show that graphene nanosheet stands perpendicularly to the substrates to form a 3D ordered and interconnected array structure, which is more clear in the tilted view (Fig. S3). TEM was used to characterize the tapered structure of the VAGNAs. As shown in Fig. 1e, it is found that the VAGNAs are continuous. HR-TEM (Fig. 1f) shows that single-layer graphene termination at the top of VAGNAs, the inset shows the schematic illustration of the VAGNAs.

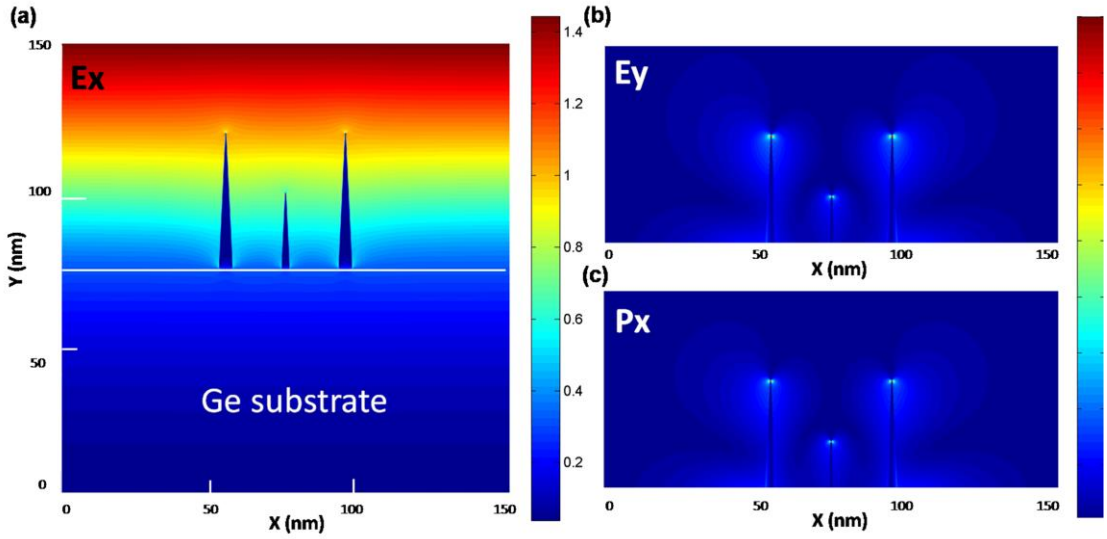

Fig. 2. Finite difference time domain (FDTD) simulation of the interaction between the incident laser and VAGNAs structure (a) incident light (Ex) interacting with the VAGNAs on Ge substrate. (b) the scattered electric field with the polarization in the y-direction. (c) the scattered energy flow distribution in the x-direction.

Raman spectroscopy has been an effective tool in identifying the presence of graphene and the number of graphene layers. However, in the case of a vertically grown graphene structure where the tip is terminated by mono or few layers of graphene, the interaction of laser and the vertical graphene (VG) structures and hence the scattered electric field and power flow is expected to be much different than that of the flat graphene layers. We have used a home-made two-dimensional finite difference time domain method (FDTD)[29] to study the interaction of the laser and structures of VAGNAs, as shown in Fig. 2a. Details of the simulation parameters are included in Supplementary Information. For the incident wavelength of 532 nm, the FDTD calculation results show that the scattered electric field and scattered energy flow are concentrated near the topping structure of the VAGNAs, as indicated by the electric

field Ey and energy flow Px in Fig. 2b-2c. Therefore, the detector in the Raman spectroscopy mainly collects the scattered light from the topping structures because of the enhanced electric field at the tip. This suggests the effectiveness of Raman data in identifying the number of terminated graphene layers, despite having multiple layers at the base of the grown VAGNAs. Henceforth, along with TEM, Raman signal has been subsequently used to identify the terminated graphene layers in the grown VAGNAs.

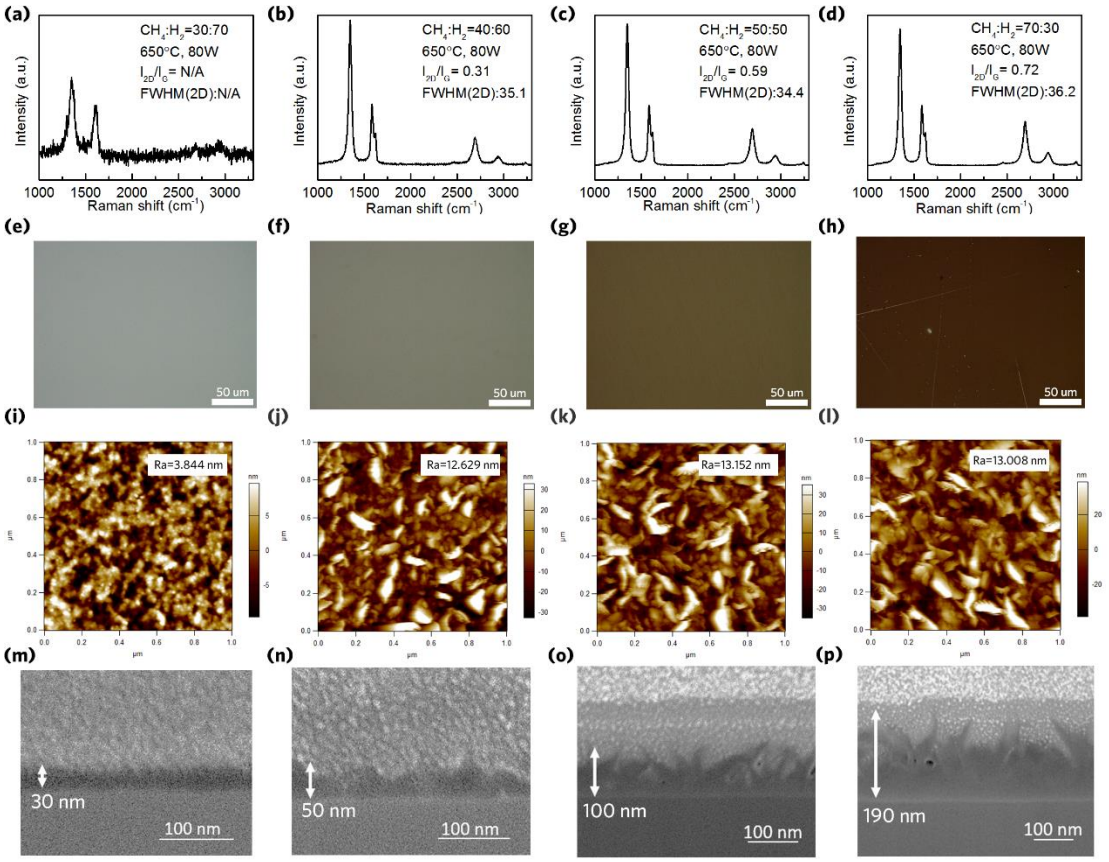

Fig. 3. The effect of CH_4/H_2 ratio on VAGNAs growth. (a)-(d) Raman, (e)-(h) optical, (i)-(j) AFM and (m)-(p) SEM are used to characterize the VAGNAs grown with CH_4/H_2 ratio of 30/70, 40/60, 50/50 and 70/30, respectively.

The effect of CH_4/H_2 ratio on the VAGNAs growth is illustrated in Fig. 3. Raman, optical, and AFM were used to characterize VAGNAs grown with different CH_4/H_2

ratios. It is found that excess H_2 does not produce VAGNAs (Fig. 3a), which shows a grey color (Fig. 3e), smooth surface (Fig. 3i) and low roughness R_a of 3.844 nm (Fig. 3i). As more CH_4 was supplied, multilayer graphene terminated VAGNAs began to form (Fig. 3b-3d). It is found that a high-intensity D peak appears in all the Raman spectra, which comes from defects such as edges, point vacancy, 5-7 ring and so on. Besides that, the existence of a shoulder D' peak located at 1622 cm^{-1} is also indicative of a defect structure.[30-33] Optical images (Fig. 3e-3h) show that as more CH_4 is introduced, the height of VAGNAs increases from 30 nm to 190 nm (Fig. 3m-3p), which leads to a color change from gray to dark brown. As confirmed by AFM (Fig. 3i-3l), the VAGNAs grown with CH_4/H_2 of 40/60, 50/50 and 70/30 exhibit similar surface topography and roughness (R_a of ～13 nm).

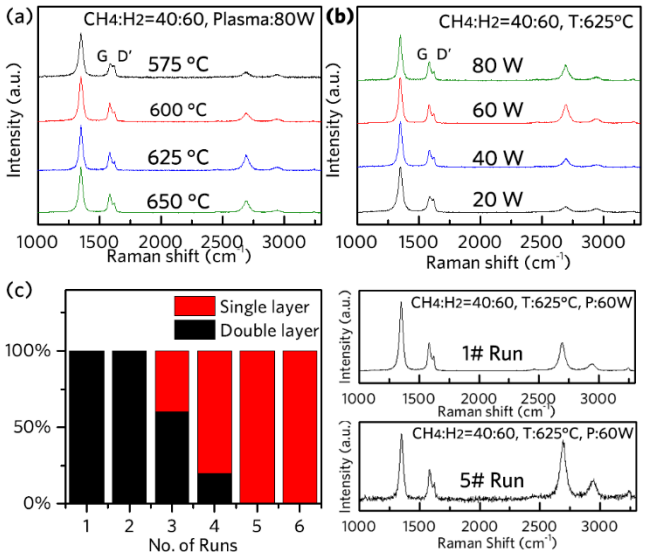

Fig. 4. Growth of single-layer graphene terminated VAGNAs. Raman spectra of VAGNAs grown with (a) different temperature and (b) plasma power. (c) Statistical percentage (10 points) of the Raman spectra with different run numbers, and the corresponding typical Raman spectra of the 1st and 5th run, respectively

To grow VAGNAs terminated with single-layer graphene, we optimized the temperature, plasma power and PECVD chamber environment, and summarized the results in Fig. 4, all the Raman peaks are normalized to G peak intensity and the relative intensity ratio of I_{2D}/I_G was used to identify the graphene thickness at the top of the VAGNAs, the I_{2D}/I_G and FWHM of 2D were summarized in Table S1 and Table S2. As shown in Fig. 4a, at a low temperature of 575℃, the high ratio of $I_{D'}/I_G$ indicates more defects.[31] At an optimal temperature of 625℃, VAGNAs with I_{2D}/I_G close to 1 indicates the presence of mainly bi-layer graphene terminated VG, whereas the non-optimized temperature of 600℃ and 650℃ produces the VAGNAs with multilayer graphene edges. It is found that the plasma power has similar effects (Fig. 4b), the optimal plasma power is found to be 60 W. In our work, we found that the PECVD chamber environment had a critical effect on the top structure of VAGNAs. Fig. 4c shows that in the first two runs, VAGNAs terminated with mainly bi-layer graphene edges can be achieved, which was also observed in TEM (Fig. S4); and in the 3rd and 4th runs, VAGNAs terminated with single-layer graphene appears; finally, from the 5th run, uniform, large-area VAGNAs terminated with single-layer graphene can be obtained. However, the sample surface becomes non-uniform after the 8th run (Fig. S5), indicating that the PECVD chamber needs to be cleaned. As more carbon gets deposited on the PECVD chamber wall and the carrier wafer (Fig. S6), the activated species adsorbed in the carbon deposits could benefit the growth of VAGNAs.[34] Wang et. al.[35] prove that the amorphous carbon deposited inside the PECVD chamber can be used as a carbon source to grow bilayer and trilayer vertical graphene on a metal

substrate. In our experiments, the single-layer graphene terminated VAGNAs can only be obtained after enough amorphous carbon deposited inside the chamber. Briefly, the intense ion bombardment introduces surface roughness that leads to defects and buckles in the buffer layers, followed with the accumulation of internal stress. Accordingly, the edges of buffer layers or defects curved upward, and the vertical growth of graphene stemmed from these curving edges. Finally, the diffusion of carbon cations along the vertical nanowall was enhanced by the local electric field in the sheath layer in plasma, which guided the vertically oriented growth of graphene.[26] The vertical graphene growth by PECVD appears to be a complex process and extensive study is needed to clarify the growth mechanism of single-layer graphene terminated VAGNAs.

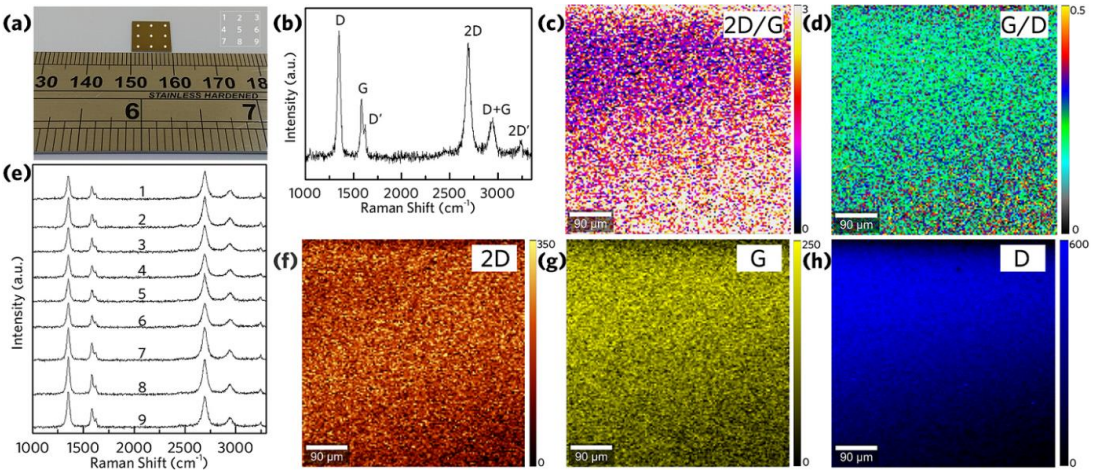

Fig. 5. Characterization of the large area, uniform single-layer graphene terminated VAGNAs. (a) Photo of a 1 cm^2 VAGNAs grown on Ge substrate, the inset shows the collection position. Raman spectra summarized in (e). (b) Typical Raman spectra of the single-layer terminated VAGNAs and the corresponding Raman mapping of the (f) 2D peak, (g) G peak and (h) D peak. Raman mapping of 2D/G and G/D were summarized in (c) and (d), respectively.

Table 1: The ratio of I_{2D}/I_G, FWHM, and position of 2D peak extracted from Fig. 5e

	I_{2D}/I_G	**FWHM of 2D (cm^{-1})**	**Position of 2D (cm^{-1})**
VAGNAs	2.2±0.2	32.3±0.4	2694±1.2
Ref. 17 [Fig. 6]	NA	36 (Si/Ni substrate)	2698 (Si/Ni substrate)
	NA	41(Si/Au substrate)	2698 (Si/Au substrate)

Raman mapping was used to examine the uniformity of the 1 cm^2 VAGNAs grown on Ge. As shown in Fig. 5a, we collected Raman spectra from 9 different points, the inset shows the collection position, the results were summarized in Fig. 5e and Table 1, all of which confirmed the single-layer graphene terminated VAGNAs. Fig. 5b shows a typical Raman spectrum of the single-layer graphene terminated VAGNAs, with a strong D peak centered at 1352 cm^{-1} indicating high defect density. Besides that, the appearance of D' peak (1622 cm^{-1}) and D+G peak (2945 cm^{-1}) is also indicative of a defect structure.[30-33] The typical I_{2D}/I_G ratio of ~2 and FWHM of 32 cm^{-1} indicate single-layer graphene at the top, and the blueshift of the 2D peak (2693 cm^{-1}) compared with exfoliated graphene on SiO_2 (2683 cm^{-1}) points to the existence of compressive strain in the graphene.[36] Raman mapping of 2D, G and D peaks shown in Fig. 5f-5h confirms a uniform VAGNAs within the scan range of 485 um×493 um. The Raman mapping of I_{2D}/I_G and I_G/I_D shown in Fig. 5c and Fig. 5d further confirm the uniformity of the VAGNAs grown on Ge. The uniformity of the Raman mapping, which is a result

of the scattering of light mainly from the tip structure, suggests that most of our VAGNAs are terminated with the same number of graphene layers.

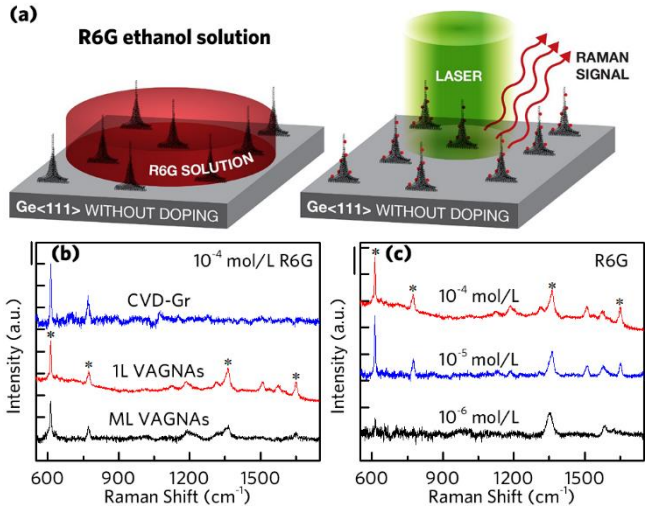

Fig. 6. VAGNAs as SERS substrate. (a) Schematic of the experimental procedure. (b) Raman intensity of R6G (10^{-4} M) on the transferred single-layer graphene grown on copper, 1L VAGNAs and ML VAGNAs. (c) Raman spectra of R6G collected from 1L VAGNAs at different concentrations of 10^{-4}, 10^{-5}, and 10^{-6} M (scale bar: 500 cps).

High-quality single-layer graphene has been used as an efficient SERS substrate due to the charge transfer between absorbed molecular and the 2D honeycomb crystal structure, which results in a chemical enhancement. Single-layer graphene exhibits a much stronger SERS effect than that of the multilayer graphene because of the more effective charge transfer process.[37] Rhodamine 6G (10^{-4} M, R6G) was used as a Raman probe to study the SERS of the VAGNAs, the characteristic peaks of R6G were labeled by an asterisk. Fig. 6a shows the schematic of our SERS experimental procedure. As shown in Fig. 6b, VAGNAs terminated with single-layer graphene (1L VAGNAs)

exhibits the strongest SERS effect, while the VAGNAs consisting of multilayer graphene (ML VAGNAs) shows a weaker SERS effect. Charge transfer is more efficient between single-layer graphene and R6G molecular than that of the multilayer graphene. In addition, the R6G molecular is more favorable to attach to the edge of single-layer graphene, which further enhances the SERS of 1L VAGNAs. Compare to the VAGNAs, the continuous single-layer graphene grown on copper and then transferred to the Ge surface (CVD-Gr) exhibits the weakest SERS effect because most of the laser energy has been absorbed by the semiconductor Ge substrate. Fig. 6c shows that the SERS sensitivity of VAGNAs can be as low as 10^{-6} M R6G.

4 Conclusions

In summary, growth parameters such as CH_4/H_2 ratio, temperature, plasma power, and chamber environment have been systematically studied and optimized. It is shown that large-area, uniform VAGNAs terminated with high-quality single-layer graphene can be directly grown on Ge surface by PECVD without catalyst at low temperature. Due to the abundant single-layer graphene edges and the clean surface, the VAGNAs can be used as an efficient SERS substrate with detection sensitivity down to 10^{-6} M R6G. We believe that VAGNAs can be further used in supercapacitors, batteries, and fuel cell catalysts in the future.

Conflicts of interest

There are no conflicts to declare.

Acknowledgments

This work was funded under the Cooperative Agreement between the Khalifa University of Science and Technology, Masdar campus, Abu Dhabi, UAE and the Massachusetts Institute of Technology, Cambridge, MA, USA, Reference Number 8474000018. M.C. acknowledges the support of the Arctic Center for Sustainable Energy (ARC), UiT Arctic University of Norway through grant no. 310059.

Appendix A. Supporting information

Supplementary data associated with this article can be found online

References

[1] P.K. Roy, G. Haider, T.-C. Chou, K.-H. Chen, L.-C. Chen, Y.-F. Chen, et al., Ultrasensitive Gas Sensors Based on Vertical Graphene Nanowalls/SiC/Si Heterostructure, ACS Sens.2019; 4(2): 406-12.

[2] S. Mao, K. Yu, J. Chang, D.A. Steeber, L.E. Ocola, J. Chen, Direct Growth of Vertically-oriented Graphene for Field-Effect Transistor Biosensor, Sci Rep.2013; 3: 1696.

[3] X. Zhang, F. Meng, S. Mao, Q. Ding, M.J. Shearer, M.S. Faber, et al., Amorphous MoSxCly electrocatalyst supported by vertical graphene for efficient electrochemical and photoelectrochemical hydrogen generation, Energy Environ Sci.2015; 8(3): 862-68.

[4] A. Malesevic, R. Kemps, A. Vanhulsel, M.P. Chowdhury, A. Volodin, C. Van Haesendonck, Field emission from vertically aligned few-layer graphene, J Appl Phys.2008; 104(8): 084301.

[5] L. Jiang, T. Yang, F. Liu, J. Dong, Z. Yao, C. Shen, et al., Controlled synthesis of

large-scale, uniform, vertically standing graphene for high-performance field emitters, Adv Mater.2013; 25(2): 250-5.

[6] H. Ci, H. Ren, Y. Qi, X. Chen, Z. Chen, J. Zhang, et al., 6-inch uniform vertically-oriented graphene on soda-lime glass for photothermal applications, Nano Res.2018; 11(6): 3106-15.

[7] J. Liu, W. Sun, D. Wei, X. Song, T. Jiao, S. He, et al., Direct growth of graphene nanowalls on the crystalline silicon for solar cells, Appl Phys Lett.2015; 106(4): 043904.

[8] Y. Yoon, K. Lee, S. Kwon, S. Seo, H. Yoo, S. Kim, et al., Vertical Alignments of Graphene Sheets Spatially and Densely Piled for Fast Ion Diffusion in Compact Supercapacitors, ACS Nano.2014; 8(5): 4580-90.

[9] Q. Liao, N. Li, S. Jin, G. Yang, C. Wang, All-solid-state symmetric supercapacitor based on Co3O4 nanoparticles on vertically aligned graphene, ACS Nano.2015; 9(5): 5310-17.

[10] T.M. Dinh, A. Achour, S. Vizireanu, G. Dinescu, L. Nistor, K. Armstrong, et al., Hydrous RuO2/carbon nanowalls hierarchical structures for all-solid-state ultrahigh-energy-density micro-supercapacitors, Nano Energy.2014; 10: 288-94.

[11] L. Shi, C. Pang, S. Chen, M. Wang, K. Wang, Z. Tan, et al., Vertical Graphene Growth on SiO Microparticles for Stable Lithium Ion Battery Anodes, Nano Lett.2017; 17(6): 3681-87.

[12] Z. González, S. Vizireanu, G. Dinescu, C. Blanco, R. Santamaría, Carbon nanowalls thin films as nanostructured electrode materials in vanadium redox flow batteries, Nano Energy.2012; 1(6): 833-39.

[13] W. Li, Z. Zhang, Y. Tang, H. Bian, T.W. Ng, W. Zhang, et al., Graphene‐Nanowall‐Decorated Carbon Felt with Excellent Electrochemical Activity Toward VO2+/VO2+ Couple for All Vanadium Redox Flow Battery, Adv Sci.2016; 3(4): 1500276.

[14] Z. Zhang, W. Li, M.F. Yuen, T.-W. Ng, Y. Tang, C.-S. Lee, et al., Hierarchical composite structure of few-layers MoS2 nanosheets supported by vertical graphene on carbon cloth for high-performance hydrogen evolution reaction, Nano Energy.2015; 18: 196-204.

[15] Z. Zhang, C.-S. Lee, W. Zhang, Vertically Aligned Graphene Nanosheet Arrays: Synthesis, Properties and Applications in Electrochemical Energy Conversion and Storage, Adv Energy Mater.2017; 7(23): 1700678.

[16] Z. Bo, S. Mao, Z.J. Han, K. Cen, J. Chen, K.K. Ostrikov, Emerging energy and environmental applications of vertically-oriented graphenes, Chem Soc Rev.2015; 44(8): 2108-21.

[17] K. Davami, M. Shaygan, N. Kheirabi, J. Zhao, D.A. Kovalenko, M.H. Rümmeli, et al., Synthesis and characterization of carbon nanowalls on different substrates by radio frequency plasma enhanced chemical vapor deposition, Carbon.2014; 72: 372-80.

[18] J. Wang, M. Zhu, R.A. Outlaw, X. Zhao, D.M. Manos, B.C. Holloway, Synthesis of carbon nanosheets by inductively coupled radio-frequency plasma enhanced chemical vapor deposition, Carbon.2004; 42(14): 2867-72.

[19] Y. Wu, P. Qiao, T. Chong, Z. Shen, Carbon Nanowalls Grown by Microwave Plasma Enhanced Chemical Vapor Deposition, Adv Mater.2002; 14(1): 64-67.

[20] Z. Bo, Y. Yang, J. Chen, K. Yu, J. Yan, K. Cen, Plasma-enhanced chemical vapor deposition synthesis of vertically oriented graphene nanosheets, Nanoscale.2013; 5(12): 5180-204.

[21] Y. Sui, Z. Chen, Y. Zhang, S. Hu, Y. Liang, X. Ge, et al., Growth promotion of vertical graphene on SiO2/Si by Ar plasma process in plasma-enhanced chemical vapor deposition, RSC Adv.2018; 8(34): 18757-61.

[22] X. Song, J. Liu, L. Yu, J. Yang, L. Fang, H. Shi, et al., Direct versatile PECVD growth of graphene nanowalls on multiple substrates, Mater Lett.2014; 137: 25-28.

[23] J. Zhao, M. Shaygan, J. Eckert, M. Meyyappan, M.H. Rummeli, A growth mechanism for free-standing vertical graphene, Nano Lett.2014; 14(6): 3064-71.

[24] M.Y. Zhu, R.A. Outlaw, M. Bagge-Hansen, H.J. Chen, D.M. Manos, Enhanced field emission of vertically oriented carbon nanosheets synthesized by C2H2/H2 plasma enhanced CVD, Carbon.2011; 49(7): 2526-31.

[25] K. Teii, S. Shimada, M. Nakashima, A.T.H. Chuang, Synthesis and electrical characterization of n-type carbon nanowalls, J Appl Phys.2009; 106(8): 084303.

[26] Y. Qi, B. Deng, X. Guo, S. Chen, J. Gao, T. Li, et al., Switching Vertical to Horizontal Graphene Growth Using Faraday Cage-Assisted PECVD Approach for High-Performance Transparent Heating Device, Adv Mater.2018; 30(8): 1704839.

[27] J.H. Lee, E.K. Lee, W.J. Joo, Y. Jang, B.S. Kim, J.Y. Lim, et al., Wafer-scale growth of single-crystal monolayer graphene on reusable hydrogen-terminated germanium, Science.2014; 344(6181): 286-9.

[28] G. Wang, M. Zhang, Y. Zhu, G. Ding, D. Jiang, Q. Guo, et al., Direct Growth of

Graphene Film on Germanium Substrate, Sci Rep.2013; 3: 2465.

[29] J.Y. Lu, Y.H. Chang, Implementation of an efficient dielectric function into the finite difference time domain method for simulating the coupling between localized surface plasmons of nanostructures, Superlattices Microstruct.2010; 47(1): 60-65.

[30] M.S. Dresselhaus, A. Jorio, M. Hofmann, G. Dresselhaus, R. Saito, Perspectives on carbon nanotubes and graphene Raman spectroscopy, Nano Lett.2010; 10(3): 751-8.

[31] A.C. Ferrari, D.M. Basko, Raman spectroscopy as a versatile tool for studying the properties of graphene, Nat Nanotechnol.2013; 8(4): 235-46.

[32] D.C. Elias, R.R. Nair, T.M.G. Mohiuddin, S.V. Morozov, P. Blake, M.P. Halsall, et al., Control of Graphene's Properties by Reversible Hydrogenation: Evidence for Graphane, Science.2009; 323(5914): 610-13.

[33] D. Liu, X. Chen, Y. Hu, T. Sun, Z. Song, Y. Zheng, et al., Raman enhancement on ultra-clean graphene quantum dots produced by quasi-equilibrium plasma-enhanced chemical vapor deposition, Nat Commun.2018; 9(1): 193.

[34] K. Liu, P. Liu, K. Jiang, S. Fan, Effect of carbon deposits on the reactor wall during the growth of multi-walled carbon nanotube arrays, Carbon.2007; 45(12): 2379-87.

[35] Z. Wang, M. Shoji, K. Baba, T. Ito, H. Ogata, Microwave plasma-assisted regeneration of carbon nanosheets with bi- and trilayer of graphene and their application to photovoltaic cells, Carbon.2014; 67: 326-35.

[36] G. Tsoukleri, J. Parthenios, K. Papagelis, R. Jalil, A.C. Ferrari, A.K. Geim, et al., Subjecting a graphene monolayer to tension and compression, Small.2009; 5(21): 2397-

402.

[37] X. Ling, L. Xie, Y. Fang, H. Xu, H. Zhang, J. Kong, et al., Can graphene be used as a substrate for Raman enhancement?, Nano Lett.2010; 10(2): 553-61.